Available online at www.sciencedirect.com
SCIENCE DIRECT®

Journal of the European Ceramic Society 23 (2003) 1761–1768

www.elsevier.com/locate/jeurceramsoc

Grain boundary phase in AlN ceramics fired under reducing N_2 atmosphere with carbon

Hiromi Nakano[a,*], Koji Watari[c], Kazuyori Urabe[b]

[a]*Electron Microscope Laboratory, Ryukoku University, Seta Otsu, 520-2194 Japan*
[b]*Department of Materials Chemistry, Ryukoku University, Seta Otsu, 520-2194 Japan*
[c]*National Institute of Advanced Industrial Science and Technology (AIST), Shimo-shidami, Moriyama-ku, Nagoya, 463-8560 Japan*

Received 29 March 2002; received in revised form 10 October 2002; accepted 28 October 2002

Abstract

An AlN ceramic was prepared with a dopant Y_2O_3 under a reducing nitrogen atmosphere with carbon at 1900 °C for 20 h. The AlN ceramic had thermal conductivity, 220 W/m°C, which contained crystalline Y_2O_3 and an amorphous intergranular film. The intergranular phase decreased during the isothermal hold period by the migration of a liquid phase that consisted of Y_2O_3, Al_2O_3, and AlN. The liquid phase composition was maintained during the firing process. Comparison of the microstructures of the ceramics prepared with different isothermal hold times revealed that the lower the quantity of intergranular phase, the higher the thermal conductivity attained.

Keywords: AlN; Electron microscopy; Grain boundaries; Nitrides; Sintering; Thermal conductivity

1. Introduction

The thermal conductivity of AlN ceramics is strongly influenced by the oxygen content in the AlN grains.[1,2] It is, therefore, relevant to reduce the oxygen content in the grains. Use of a high-purity powder,[3] addition of useful sintering aids to decrease oxygen content in the grains through precipitation of grain-boundary crystalline phase or phases,[4–6] and sintering under a reducing N_2 atmosphere with carbon,[7–10] are effective methods to enhance conductivity. In particular, significant improvement results from firing under a reducing N_2 atmosphere with carbon at above 1800 °C. After this process, the conductivity easily reached values higher than 200 W/m°C at room temperature.[7–10]

In sintering of Y_2O_3 doped AlN ceramics under a reducing N_2 atmosphere with carbon, the following reactions occur, which cause a decrease in the oxygen content [10]:

$$Al_2Y_4O_9 + N_2 + 3C \rightarrow 2Y_2O_3 + 2AlN + 3CO \quad (1)$$

$$Y_2O_3 + N_2 + 3C \rightarrow 2YN + 3CO \quad (2)$$

During the reactions, the yttrium in an AlN sintered body moves to the surfaces of the sample to form $Al_2Y_4O_9$, Y_2O_3, and YN. The migration of grain-boundary phases was investigated in detail by Yagi and Shinozaki [9]. They reported that $Al_2Y_4O_9$ decomposed into Y_2O_3 and Al_2O_3, which migrated toward the surface of a specimen, and that those oxides were nitrided to form a surface layer of YN and AlN [9]. In this case, concentration gradients of the elements such as Y, Al, N and O were also observed from the center of the sintered body to its surface.

Recently, the authors obtained an AlN ceramic with thermal conductivity as high as 272 W/m°C by long-term (100 h) firing at 1900 °C under a reducing atmosphere.[11,12] This value was slightly lower than that of the maximum conductivity of a single crystal (285 W/m°C), and reached 85% of the intrinsic conductivity (320 W/m°C) of AlN. Most of the grains appeared to be in direct contact with each other, resulting in the

* Corresponding author. Tel.: +81-77-543-7774; fax: +81-77-543-7749.
E-mail address: hiromi@rins.ryukoku.ac.jp (H. Nakano).

0955-2219/02/$ - see front matter © 2003 Elsevier Science Ltd. All rights reserved.
PII: S0955-2219(02)00408-9

formation of triple-grain junctions with no intergranular phase. However, the microstructural characterization of the specimen proved that a grain boundary film was to be found between two grains with a thickness of less than 1 nm.[12] Furthermore, the concentrations of yttrium and oxygen atoms, which existed as grain boundary elements, were reduced to 0.05 and 0.03 mass%, respectively.

In the present work, an AlN ceramic was prepared by firing at 1900 °C for 20 h under a reducing N_2 atmosphere with carbon and the grain boundaries and triple junctions of the specimen were newly investigated with high-resolution transmission electron microscopy (HRTEM). The result was then compared to that of the AlN ceramic fired at 1900 °C for 100 h in order to clarify the microstructural evolution during the holding. New evidence about the microstructural evolution of AlN ceramics during isothermal holding at 1900 °C was described.

Table 1
Characterization of AlN ceramics fired at 1900 °C for 20 and for 100 h

Sintering conditions	Density (kg/m^3)	Chemical composition		Grain boundary phase	Thermal conductivity (W/m°C)
		Oxygen (mass%)	Yttrium (mass%)		
1900 °C, 20 h	3281	0.14	0.20	None	220
1900 °C, 100 h	3260	0.05	0.03	None	272

2. Experimental procedure

The experimental procedure for the fabrication of a polycrystalline AlN specimen with a high conductivity was described in detail elsewhere;[11] it is mentioned only briefly here. One mole% (5.2 mass%) of a Y_2O_3 powder was added to a raw AlN powder (Tokuyama, Japan). The oxygen impurity in the AlN powder was of the level of 0.8 mass%. After mixing and drying, the mixture was pressed into rods, and then cold isostatically pressed (CIPed). The rods were fired in a tungsten resistance furnace at 1800 °C for 1 h under a N_2 gas pressure of 0.1 MPa. After this process, the product was placed in a carbon container for firing in a reducing N_2 atmosphere at 1900 °C for 20 h.

The surface layer of the specimen was removed, and taken for chemical analysis. A commercial hot gas extraction analyzer (TC-136, LECO Co.) was employed to measure the oxygen content in the AlN grains and the total oxygen content in the fired sample. Density measurements were performed by the Archimedes method in distilled water. Phase composition of the sample was identified by X-ray diffractometry (XRD). Thermal conductivity at room temperature was measured by a laser flash technique[10,11].

TEM foil was prepared by using an Ar-ion thinning technique after mechanical thinning and dimpling. Triple pockets and grain boundary films were analyzed by a TEM device (JEM-3000F, Jeol, Japan) equipped with a field emission gun. The lattice defects in AlN grains were observed by a two-beam technique and some of the crystalline phases at triple pockets were identified by the selected area diffraction (SAD) method using a TEM device (JEM-2000EX, Jeol, Japan).

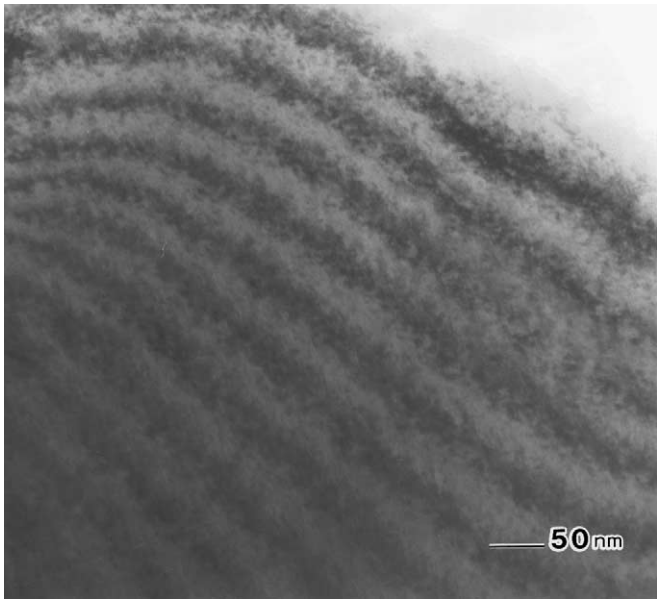

Fig. 1. TEM image of AlN grain recorded using a two-beam technique. No defect structure is observed in the grain.

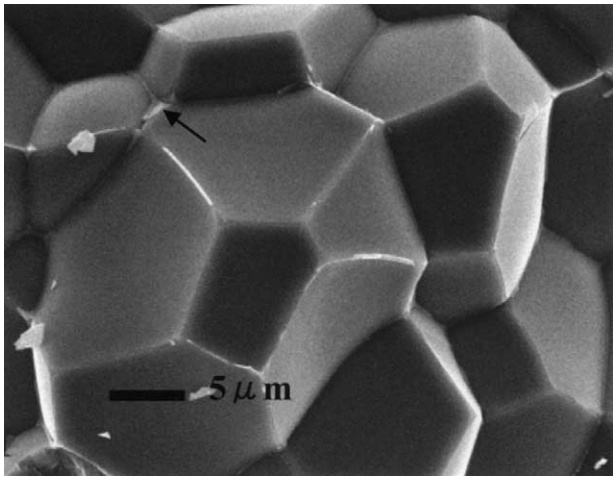

Fig. 2. SEM image of AlN ceramic showing grain boundary phase on edges of crystals.

3. Results and discussion

3.1. Properties of the AlN ceramic

Table 1 shows bulk density, total oxygen and yttrium contents, grain boundary phases, and thermal conductivity for the AlN sintered body fired at 1900 °C for 20 h together with the value for the specimen fired for 100 h for ease of comparison. The bulk density was not improved by firing for 100 h; however, the thermal conductivity was enhanced significantly when the hold time was prolonged. Among the properties that are listed in Table 1, oxygen and yttrium contents were in a reverse proportional relation to the thermal conductivity.

Providing that all of the yttrium atoms form a sesquioxide, Y_2O_3, in the specimen, about 40% of the oxygen atoms (0.056 mass% in the bulk composition) are consumed and the volume fraction of Y_2O_3 was estimated to reach about 0.18% in the specimen. The remaining oxygen atoms (0.084 mass% in the bulk composition) exist in the lattice points in AlN replacing N atoms and/or in intergranular films.

Fig. 1 shows a TEM micrograph of an AlN grain recorded by using the two-beam technique. No contrast caused by lattice defects was recorded on the crystal. The oxygen atoms that were incorporated in the AlN were estimated to be about 0.1 mass% when no intergranular phase other than Y_2O_3 existed. The vacancies that were caused by oxygen atoms of this concentration level do not contribute to form either a dislocation or a stacking fault that was detectable by TEM, although contrasts due to dislocations and stacking faults were reported in the AlN specimens with higher oxygen concentrations by Hagege et al.[13] and Harris et al.[14].

3.2. Microstructure in the grain boundary region

Fig. 2 shows a scanning electron microscopic (SEM) image of the specimen. An intergranular phase was observed as segments with a bright contrast along the edges of AlN grains and as distorted triangles around some of the apices where the edges of three grains crossed, the latter being indicated by the arrow in Fig. 2. This type of microstructure suggested that the intergranular phase made a continuous network through the ceramic body, which acted as a path for the material oozing out to the surface.

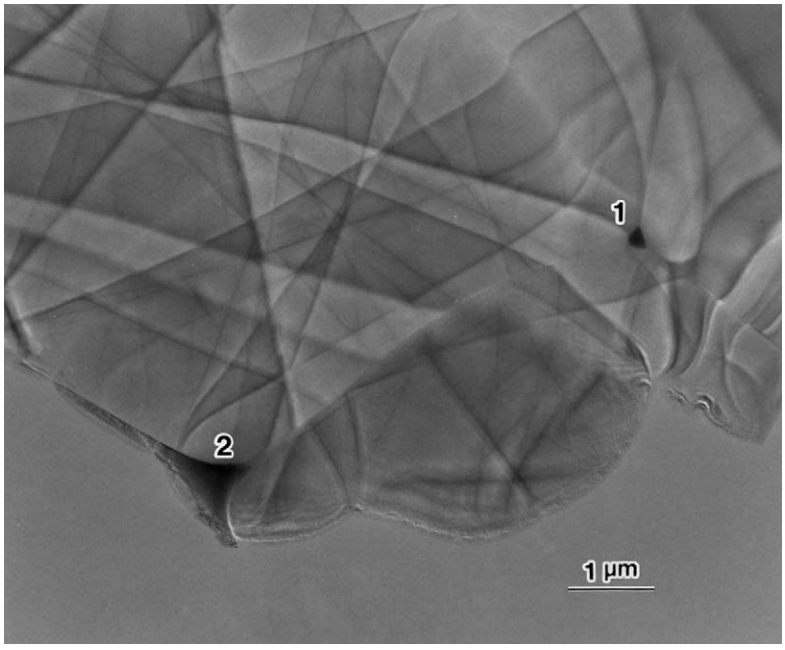

Fig. 3. TEM micrograph of AlN ceramic. The triple pockets are composed of Y_2O_3 crystals.

Fig. 3 shows a low-magnification TEM image of the specimen. The intergranular phase was found at triple junctions, as indicated by numbers. A discrete particle with a dihedral angle of about 120° was found at one of the junctions marked by (1) and a grain boundary phase marked by (2) continued to two-grains junctions. Both of them were identified to be a crystalline phase of Y_2O_3.

Fig. 4 shows TEM images of a typical discrete type of Y_2O_3 crystal at a triple junction in (a), and a two-grain junction oriented in an edge-on condition in (b). Inset is a SAD pattern obtained from the Y_2O_3 crystal normal to the [110]. The intergranular film found in the two-grain junction appeared as a channel of darker color and had no lattice fringe. This fact indicated that the film consisted of amorphous material, whose thickness was about 1.2 nm. The value was wider than that observed in the specimen held for 100 h at 1900 °C.[12]

The point analysis of the Y_2O_3 crystal and the distribution of elements Y and Al along a line across the channel in Fig. 4 are given in Fig. 5. The Y_2O_3 crystal exhibited strong peaks for Y and O. The intergranular film also contained elements Y and O, and the former was distributed in the boundary region with a width of 6 nm, which was wider than the thickness of the film in Fig. 4(b) due to the irradiated electron beam scattered over the width of the film. This result indicated that most of the Y component in the bulk composition was in the crystalline form of Y_2O_3 and a small amount of the element existed in the amorphous film.

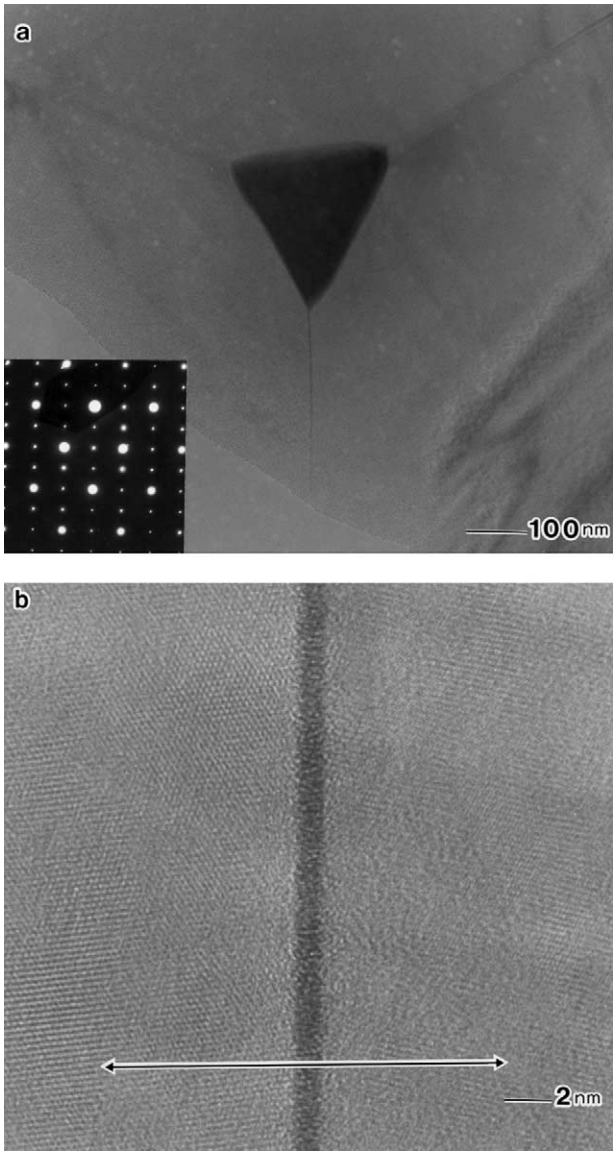

Fig. 4. TEM image of AlN ceramic, (a) Y_2O_3 crystal at triple-grain junction, (b) Two-grain boundary showing amorphous intergranular film. Inset is a SAD pattern of Y_2O_3 crystal recorded at the triple pocket.

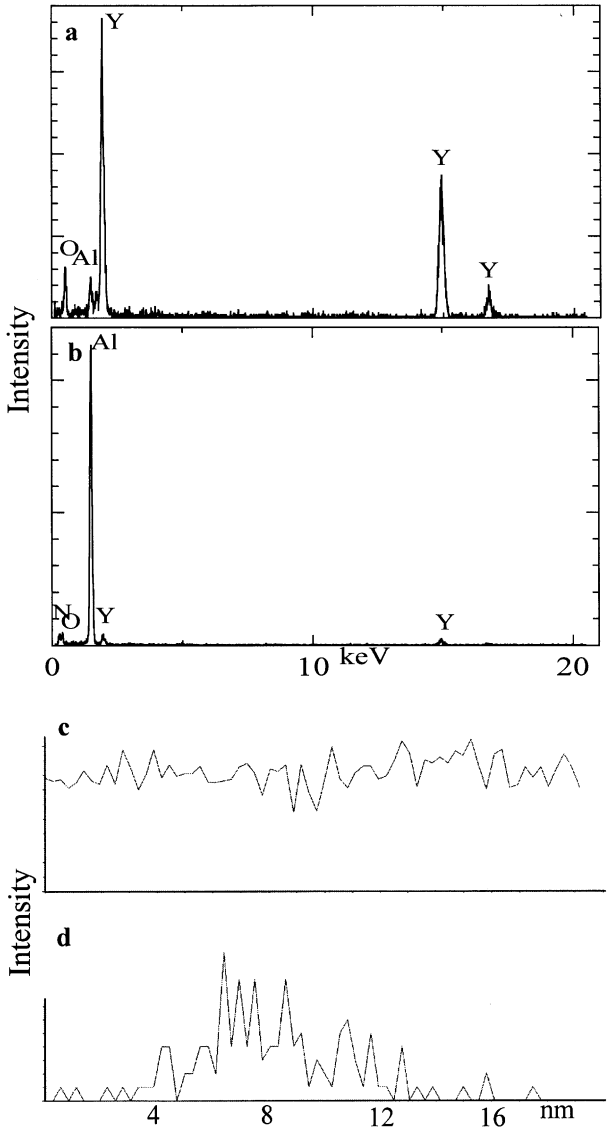

Fig. 5. EDS spectrum of AlN ceramic. (a) triple-grain junction, (b) two-grain boundary, (c) line profiles along the segment across the two-grain boundary showing distributions of Al element, and (d) that for Y element.

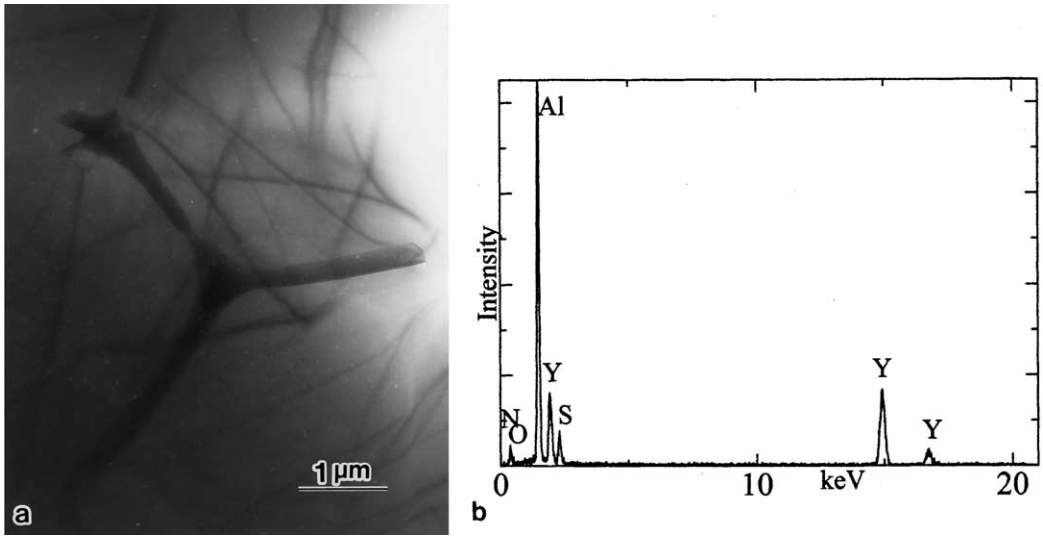

Fig. 6. (a) TEM image of a triple-grain junction, and (b) EDS spectrum at the center of the triple pocket showing a peak for S element.

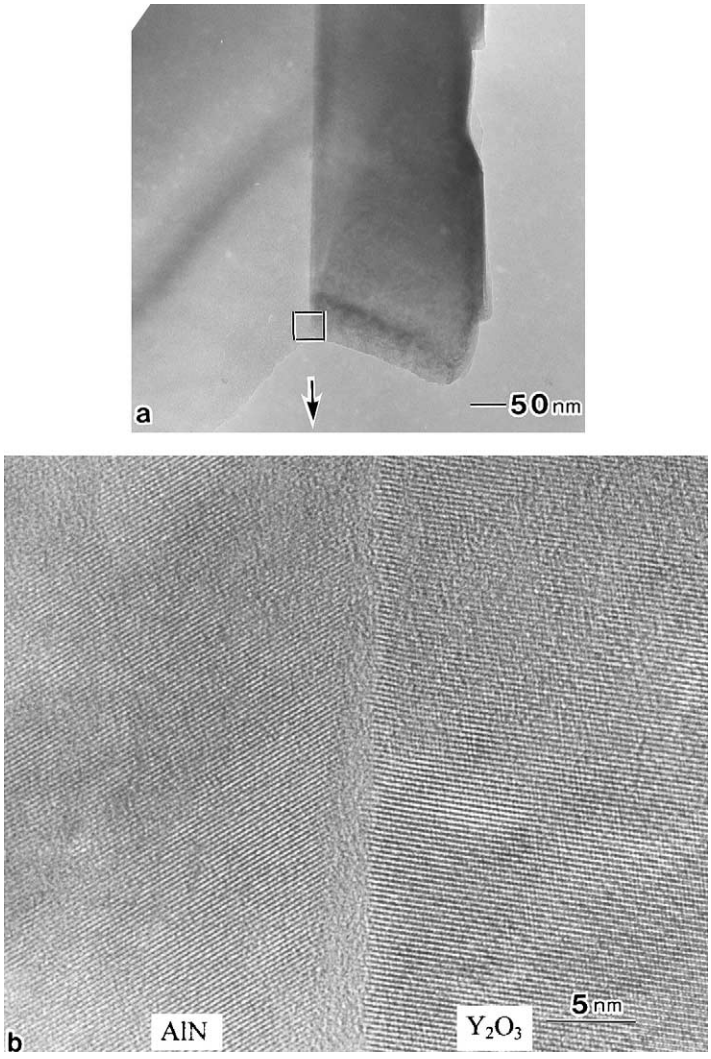

Fig. 7. TEM micrographs of AlN ceramic, (a) low-magnification TEM image, and (b) HRTEM image showing intergranular film between the two crystals.

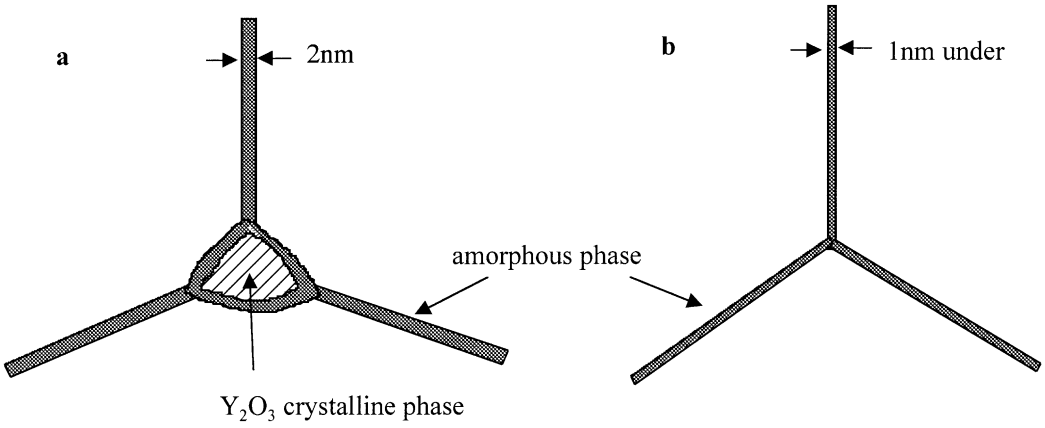

Fig. 8. Microstructural model of AlN ceramics fired at 1900 °C for (a) 20 h, and (b) 100 h.

In the AlN ceramic fired for 100 h, most of the grains seemed to be in direct contact with each other, but a special triple junction possessed a crystalline phase that contained element S in addition to Y, O, Al, and N.[12] Such a special compound has rarely been found in this specimen. Fig. 6 shows a TEM image of the region, (a), and the EDS spectrum obtained from the center of the triple junction, (b). The S component was detected from only the center of the triple pocket. The origin of the S-containing compound was still uncertain. However, it was suggested that a low solubility of the compound with the intergranular liquid prevented the compound from migrating to the surface of the ceramic, which caused the component to remain in the ceramic even though the concentration was very low.

Fig. 7 shows a grain boundary between AlN and Y_2O_3. The darker region in (a) consists of a Y_2O_3 crystal and the square is part of the grain boundary, a detail of which is given in (b). Lattice fringes, which could be traced near the grain boundary for both of the crystals, were clearly observed in (b). However, an amorphous phase of 1–4 nm in thickness was recognized between the two crystals.

The microstructural evidence that was newly clarified in the specimen is summarized in the schematic illustration, which is shown in Fig. 8 (a). A similar illustration in Fig. 8 (b) is for the microstructure of the AlN ceramic held for 100 h at 1900 °C.[12] All the grains observed in both AlN ceramics were in contact with each other with an amorphous grain boundary film between them, which contained Y and O in addition to Al and N. The difference in the microstructures of the two ceramics was in the amount of crystalline Y_2O_3 and the thickness of the interlayer film. The equilibrium film thickness may be affected by the atomistic structure of the grain boundary glass, as seen in Si_3N_4. [15]

Fig. 9 shows bulk compositions of the ceramics fired at 1900 °C for 20 h, that fired for 100 h, and the starting mixture. Since the starting mixture contained 5.2 mass% of Y_2O_3 and 0.8 mass% of O, (1.7 mass% of Al_2O_3), the bulk composition was plotted at point (a) in the three-phase diagram with the apices of AlN, Al_2O_3, and Y_2O_3. Whereas the bulk compositions of the specimens held for 20 h, and for 100 h, are plotted at points (b) and (c) respectively, both of which lie near the line passing through the composition point of AlN and the point (a). This fact indicated that the ratio of Al_2O_3 and Y_2O_3 in the specimens was maintained during the annealing process. Therefore, the decrease in oxygen impurity and Y_2O_3 was achieved mainly by the migration of the liquid phase without change in its composition during the annealing process. In the case where the reducing atmosphere influences the decrease of oxygen atoms, the bulk composition of the ceramics should be positioned in the left-side region of the line that joins AlN and the starting composition, because oxygen content decreases by the reduction reaction, as represented by Eq. (2). The line connecting points (b) and (c) in Fig. 9 crossed one of the segments of the triangle at the point of 0.075 mass% of Al_2O_3. This point was deduced to be the composition of an AlN solid solution that was in an equilibrium condition at 1900 °C, under which the solid solution and the liquid coexisted.

The Y_2O_3 crystals found in the ceramic had textures that seemed to be molded by the AlN crystals; in other words, they occurred in the grain boundary regions which the liquid phase was expected to occupy at the firing temperature (see Figs. 3, 4, and 6). This microstructural evidence suggested the following crystallization process took place on cooling: crystallization of an AlN solid solution proceeds at grain boundary regions so that AlN grains grow and the Y_2O_3 component subsequently crystallizes from the liquid phase, which fills the space in the grain boundary regions and the residual liquid concurrently forms an intergranular film.

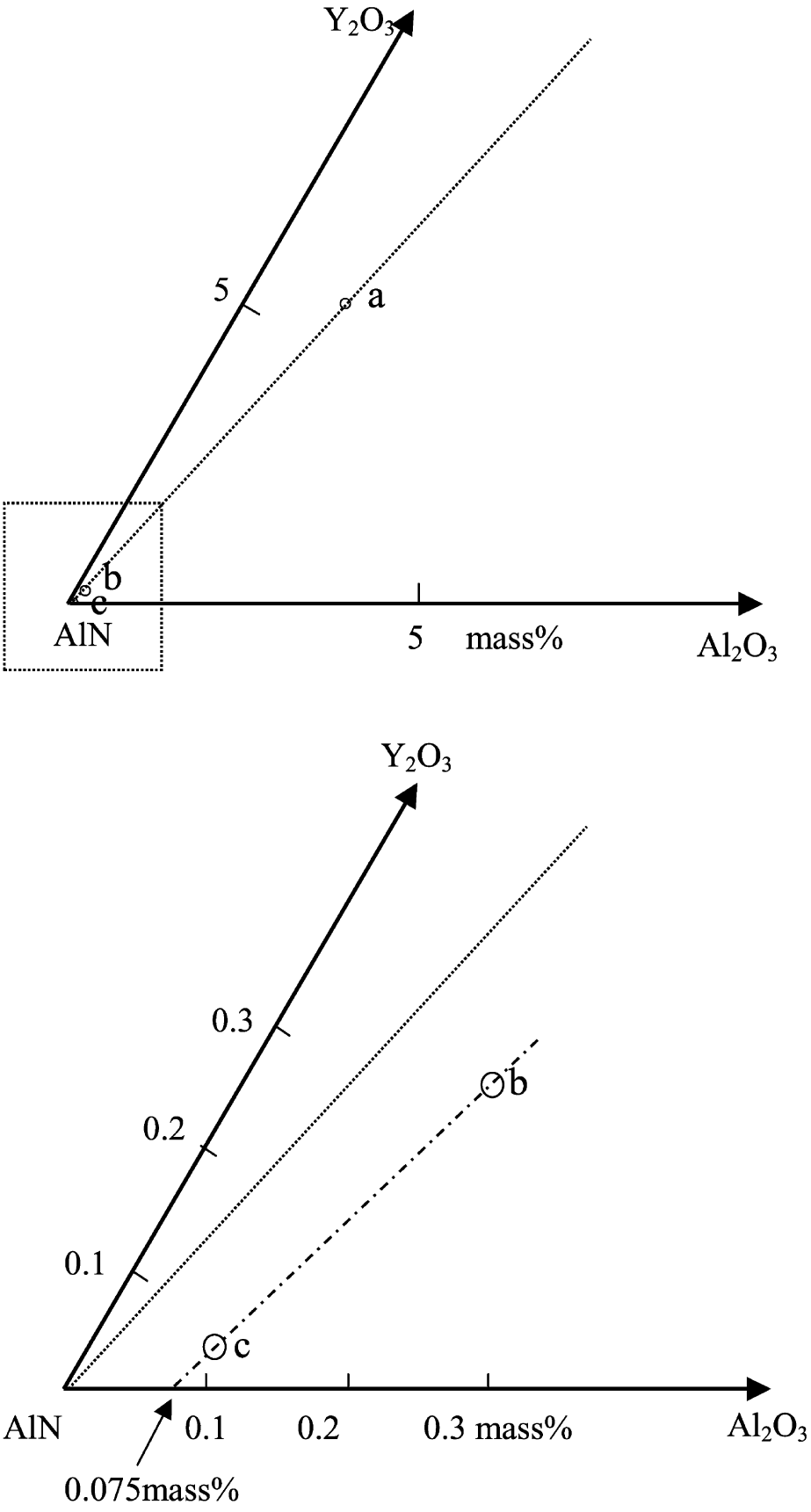

Fig. 9. Effect of hold time on bulk composition. The bulk compositions of the starting mixture in (a), and specimens held for 20 h in (b) and for 100 h in (c).

4. Conclusions

An AlN ceramic with a dopant Y_2O_3 was produced under a reducing N_2 atmosphere at 1900 °C for 20 h. Thermal conductivity of the ceramic was as high as 220 W/m°C. The microstructure of the ceramic was characterized using TEM, EDS, and oxygen impurity analysis. The results were compared with those of the AlN ceramic with thermal conductivity of 272 W/m°C. The microstructural differences between the two ceramics were in the amount of crystalline Y_2O_3 and in the thickness of the intergranular film. A model for microstructural evolution during the annealing process was as follows. A liquid phase was produced by the reaction between Al_2O_3, Y_2O_3, and AlN, which migrated to the surfaces of the ceramics without changing its composition during the isothermal holding period. Y_2O_3 and an AlN solid solution crystallize from the liquid with concurrent formation of an intergranular film in the grain boundary regions. The lower the quantity of intergranular phase, the higher the thermal conductivity attained.

References

1. Salck, G. A., Tanzilli, R. A., Pohl, R. O. and Vandersande, R. O., The intrinsic thermal conductivity of AlN. *J. Phys. Chem. Solids*, 1987, **48**, 641–647.
2. Watari, K., Ishizaki, K. and Fujikawa, T., Thermal conduction mechanism of aluminium nitride ceramics. *J. Mater. Sci.*, 1992, **27**, 2627–2630.
3. Taniguchi, H. and Kuramoto, N., Recent progress in aluminum nitride powder. *Ceramics*, 1991, **26**(8), 733–737 (in Japanese).
4. Komeya, K., Inoue, H. and Tsuge, A., Effect of various additives on sintering of aluminum nitride. *J. Ceram. Soc. Jpn.*, 1981, **89**, 58–64 (in Japanese).
5. Virkar, A. V., Jackson, T. B. and Cutler, R. A., Thermodynamic and kinetic effects of oxygen removal on the thermal conductivity of aluminum nitride. *J. Am. Ceram. Soc.*, 1989, **72**, 2031–2042.
6. Watari, K., Hwang, H. J., Toriyama, M. and Kanzaki, S., Effective sintering aids for low-temperature sintering of AlN ceramics. *J. Mater. Res.*, 1999, **14**, 1409–1417.
7. Okamoto, M., Arakawa, H., Oohashi, M. and Ogihara, S., Effect of microstructure on thermal conductivity of AlN ceramics. *J. Ceram. Soc. Jpn.*, 1989, **97**(12), 1478–1485 (in Japanese).
8. Ueno, F., Horiguchi, A., Grain boundary phase elimination and microstructure of aluminum nitride. *Proceedings of 1st European Ceramics Society Conference*, Elesevier Applied Science, London, New York (1989) 383–387.
9. Yagi, T., Shinozaki, K., Kato, M., Sawada, Y. and Mizutani, N., Migration of grain boundary phase of AlN ceramics on joined sample of sintered and hot-pressed body. *J. Ceram. Soc. Jpn*, 1990, **98**, 198–203.
10. Watari, K., Kawamoto, M. and Ishizaki, K., Sintering chemical reactions to increase thermal conductivity of aluminum nitride. *J. Mater. Sci.*, 1991, **26**, 4727–4732.
11. Watari, K., Tsugoshi, T., Nagaoka, T. Evaluation of some properties in high thermal conductivity aluminum nitride. in *Proceeding of the 18th International Japan–Korea Seminar on Ceramics* (18th International Japan–Korea Seminar on Ceramics, Kagoshima, Japan, November 21 2001) pp. 98–101.
12. Nakano, H., Watari, K., Hayashi, H. and Urabe, K., Microstructural characterization of high thermal conductivity AlN ceramics. *J. Am. Ceram. Soc.* (in press).
13. Hagege, S., Tanaka, S. and Ishida, Y., Structural analysis of planar defects in wurtzite type aluminum nitride. *J. Jpn. Inst. Metals*, 1988, **52**(12), 1192–1198 (in Japanese).
14. Harris, J. H., Youngman, R. A. and Teller, R. G., On the nature of the oxygen-related defect in aluminum nitride. *J. Mater. Res.*, 1990, **5**(8), 1763–1773.
15. Kleebe, H.-J., Structure and chemistry of interfaces in Si_3N_4 ceramics, studied by transmission electron microscopy. *J. Ceram. Soc. Jpn.*, 1997, **105**(6), 453–475.